Hardness and Indentation Size Effect in Cubic Boron Nitride Materials (BL and BH Groups)

Stepan Pavlov[1], Andrey Yurkov[2,*] and Mikhail Andrianov[3]

[1]*Russian Mendeleev University of Chemical technology, 125047 Moscow, Russia*

[2]*Russian Mendeleev University of Chemical technology, 125047 Moscow, Russia*

[3]*Microbor LLC, 109316 Moscow, Russia*

Abstract: This paper investigates the hardness and indentation size effect (ISE) in cubic boron nitride (cBN) materials, specifically focusing on two groups: BL (below 70 vol.% cBN) and BH (more than 70 vol.% cBN). The study examines the load dependence of hardness in both groups, determining the load at which hardness becomes constant. Fracture toughness, (by the length of the crack) around indentations, is also evaluated for load dependence. The materials were synthesized using different additive combinations (Al, TiC, TiN, Mo) and sintered under high pressure and temperature. Hardness was measured using a Vickers indenter, and the ISE was analyzed using Meyer's law and the proportional sample resistance (PSR) model. Fracture toughness was calculated using the Niihara equation. Results show a significant ISE in BL materials, while BH materials exhibit less “load-hardness” dependence.

Keywords: Cubic Boron Nitride (cBN), Ceramic bonding phase, Vickers Hardness, Indentation Size Effect (ISE), Fracture Toughness, Thermal Conductivity, Meyer's Law, Proportional Sample Resistance (PSR) model, High Pressure High Temperature (HPHT) sintering.

1. INTRODUCTION

Cubic boron nitride-based cutting tools are used for grinding hard ferrous alloys [1]. The atoms of boron and nitrogen in cubic boron nitride are linked by covalent bonds; sintering and processing boron nitride require temperatures above 2000 °C and pressures above 7 GPa [2]. The structure is very similar to carbon atoms in diamond, but the remarkable feature of cubic boron nitride (cBN) is its stability in air and relative inertness to ferrous alloys up to 1200 °C, while diamond starts to oxidize and graphitize at approximately 900 °C [3].

The standard procedure in processing cBN cutting tools involves the addition of additives (often with low melting points) to enhance sintering and improve mechanical properties. These additives are elements from groups IV-VI of the periodic table and compounds containing these elements [4, 5].

According to the classification and content of bonding additives, cBN materials are categorized into BL and BH groups of cBN cutting tools [6].

BL group cutting tools (below 70 vol.% of cBN) are used for grinding hardened steel and hard alloys (ISO513:2019). Additives include Al, TiN, TiC, Ti(C, N). Sometimes Ni, Co, AlB_2, or AlN are also used. The addition of metals promotes high fracture toughness.

BH group cutting tools (more than 70 vol.% of cBN) are used for surface finishing of alloys (relatively low mechanical loads and relatively high temperatures). The addition of borides, carbides, and nitrides provides high thermal stability.

Generally, there are two types of bonding additives – metals and ceramics. Metal bonding phases have high thermal conductivity and high fracture toughness but become soft at high temperatures. Ceramic bonding phases in cBN cutting tools have high hardness and thermal stability but are brittle and have low thermal conductivity.

Aluminum is a typical metal bonding phase in cBN cutting tools. Publications on Al-cBN compositions show that reactions occur between aluminum and cBN, producing new ceramic phases AlN and AlB_2. These may promote good bonding between cBN grains and the ceramic matrix [7, 8].

Titanium, when added as a bonding phase to cBN, is quite reactive and readily reacts with cBN grains, forming titanium nitride (TiN) and titanium boride (TiB_2). TiN and TiB_2 phases have good thermal stability and high hardness [9].

Recently, a new cBN-based material was produced in the cBN–Al–HfC system [10]. cBN reacts with Al and HfC, yielding AlN, AlB_2, HfB_2, and $B_2C_5N_2$ compounds. A composite made in the cBN–TiC system exhibits excellent wear resistance [11]. The microstructure and mechanical properties of cBN–TiC compounds have also been investigated, and a two-stage sintering process has been proposed to improve the mechanical properties of the composite material [12]. Recently, cBN-based products were obtained from the cBN–TiC

*Address correspondence to this author at the Russian Mendeleev University of Chemical technology, 125047 Moscow, Russia; E-mail: and-yur@mail.ru

composition at 7.7 GPa and 2000 °C with the formation of Ti(C, N) and TiB_2 [13].

The traditional hardness measurement procedure involves applying a fixed load to a diamond indenter and measuring the length of the indent diagonal after load release. At low loads, measured hardness values are usually higher than at high loads. This phenomenon is called the Indentation Size Effect (ISE), and there are different viewpoints on its origin [14]. Researchers have attempted to account for the friction component of hardness at low loads and the contribution of excessive surface energy to the hardness value at low loads.

This paper aims to investigate the load dependence of the hardness of cBN materials with a high content of additives (BL group) and with a low content of additives (BH group), to determine the loads at which hardness becomes constant (independent of load), and to evaluate whether the fracture toughness of cBN materials (measured by cracking around the indent) of both groups depends on the indenter load.

The approach of the paper is to investigate the load dependence of hardness of cBN materials with high content of additives (BL group) and with low content of additives (BH group), to evaluate the values of load on indenter, when the values of the hardness become constant (do not depend on load), to evaluate, if fracture toughness of cBN materials (measured on cracking around indent) of both groups depend on load on indenter

2. MATERIALS AND METHODS

2.1. Materials

The initial components used were: cubic boron nitride (1-3 μm, China), titanium carbide (40-60 nm, China), titanium nitride (100-200 nm, China), aluminum (800 nm, Russia), molybdenum (70 nm, China).

This stage of the work involved the investigation and comparison of experimental cutting materials with low (BL group) and high (BH group) cBN content, differing in the type and amount of additive. For BL material, the cBN content is approximately 46 vol. %, for BH – 82 vol. %. The compositions of the binder components are given below (Table **1**):

Table 1: The Content of Additives in the Syncretized cBN Materials of BL and BH Groups

Sample	Binder Phase
BL materials	Al, TiC, TiN, Mo (54 vol. %)
BH materials	Al, TiC (18 vol. %)

The synthesized BL group materials contained 54 vol.% of additives, while the BH group materials contained 18 vol.% of additives.

The powders were mixed in a paraffin-petroleum ether solution using an ultrasonic mixer. The drying of the resulting slurry was carried out in a spray dryer in a nitrogen atmosphere to obtain aggregative stable spherical particles (granules) (Figure **1**), which are conglomerates of the mixture of raw material components introduced into the charge. As clearly seen from Figure **1**, ultrasonic mixing with the selected plasticizer and drying conditions provide sufficiently uniform mixing of components that are heterogeneous both in chemical composition and dispersity.

The powder mixture was uniaxially pressed into tablets with a diameter of 36 mm at a pressure of 400 MPa in a steel die with a cemented carbide insert. High-pressure high-temperature sintering was performed in a six-anvil apparatus in a pyrophyllite container at 4.5 GPa and 1400–1450 °C for 5 minutes.

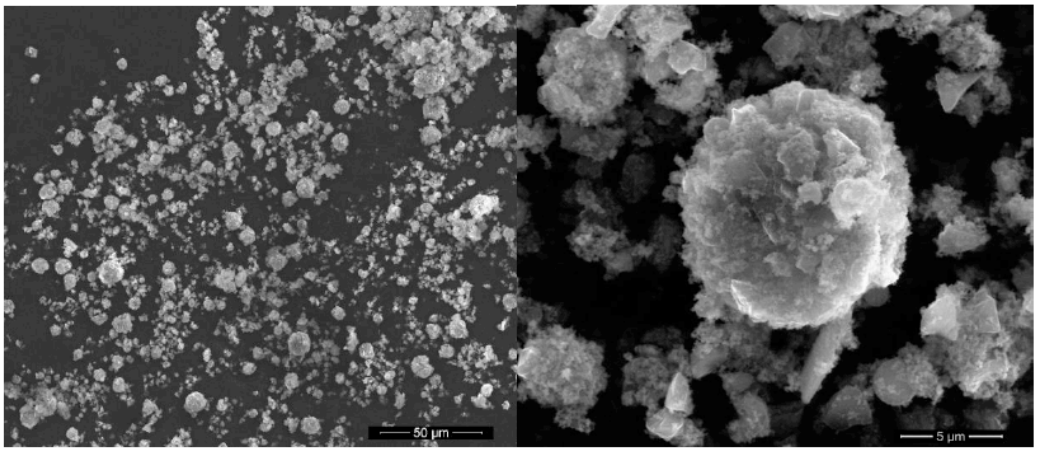

(**a**) (**b**)

Figure 1: Microstructure of the powder mixture after spray drying: a) 1000x; b) 30000x.

2.2. Analytical Procedures and Equippment

Vickers hardness was determined on a Durascan g20 hardness tester at loads of 0.5, 1, 2, 2.5, 3, and 5 kg (15-second load application) according to ASTM E384.

Fracture toughness was calculated according to the Niihara equation [15].

Structures were analyzed using a Helios NanoLab 650 scanning electron microscope in BSE mode. XRD analysis was performed using a Genesis Apex Energy Dispersive Spectroscopy System and a D8 Advance AXS (Bruker) diffractometer.

For microhardness determination, samples with d = 25 mm and h = 3.15 mm were prepared. The indentation zone after indentation was recorded using an OLYMPUS BX51 optical microscope at 50x magnification (Figure **2**).

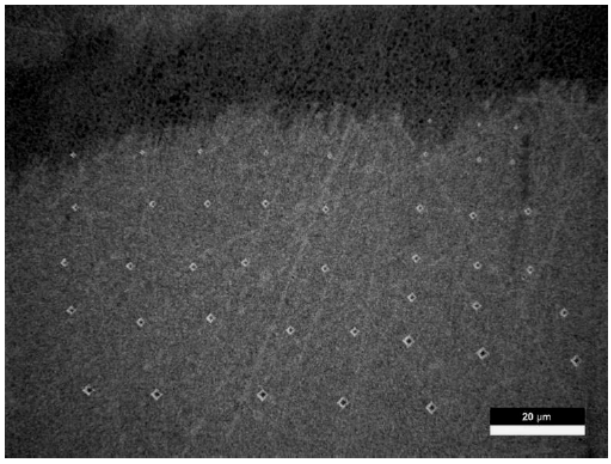

Figure 2: Optical image of the indentation area by a Vickers pyramid of the BL composition at loads of 0.5; 1; 2; 2.5; 3; 5 kgf .

Vickers hardness measurements (Hv/GPa) were performed according to the international standard ASTM E384. Hardness was calculated using formula (1):

$$H_V = 1.8544\frac{P}{d^2}, \quad (1)$$

where P is the applied load (N); d is the average of the lengths of the two diagonals for Vickers indentation (μm).

Measurements were performed at loads of 0.5; 1; 2; 2.5; 3; 5 kgf on a Durascan g20 microhardness tester using a Vickers indenter with a four-sided pyramid angle of 136° for 15 s (Figure **4**).

Fracture Toughness K_{Ic} (MPa·m$^{1/2}$) was calculated using equation (2) based on the half-length of the cracks (c, μm) formed at the corners of the indentations [16, 17]:

$$K_{Ic} = 0.016\left(\frac{E}{H}\right)^2 \frac{P}{c^{\frac{3}{2}}} \quad (2)$$

where E is the elastic modulus of the cBN-based material (GPa) [18];
c is the average half-length of the cracks (μm).

3. RESULTS

The synthesized materials of BL and BH groups have different content of cBN and different structure. The microstructure of the BL material (46 vol.% cBN) showed approximately 50 vol.% of dark cBN grains (700 nm to 2.5 μm) within a matrix of darker gray and white areas (Figure **3a**). The BH material (82 vol.% cBN) consisted of 80 vol.% cBN grains bonded by ceramic components of the matrix structure (Figure **3b**).

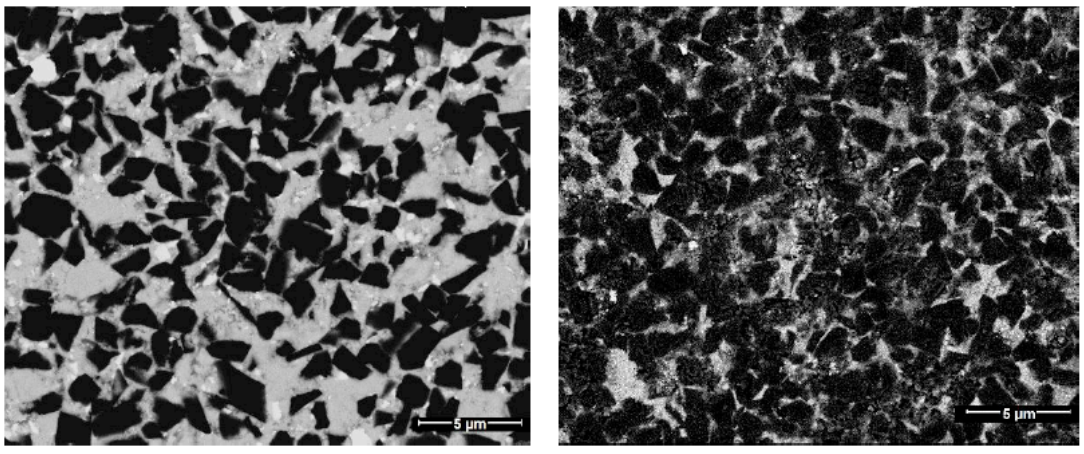

(**a**) (**b**)

Figure 3: SEM images of experimental compositions: a) BL material, 46 vol% cBN grains; b) BH material, 82 vol% cBN grains. Magnification 5000x.

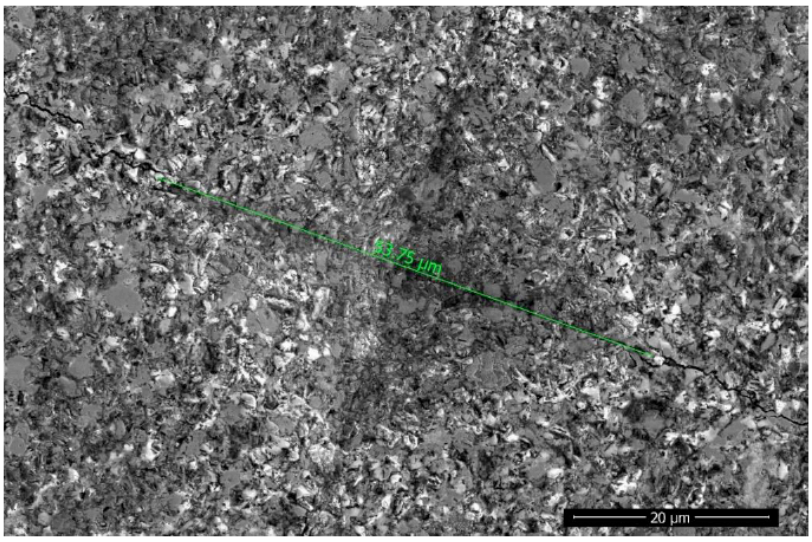

Figure 4: SEM image of the BL material indentation. Load 5 kgf. Magnification 2500x.

During the hardness measurements the so-called "indentation size effect" (ISE) of hardness is observed - at low loads there is a significant dependence of hardness on load (as the load increases, the hardness decreases, the dependence gradually reaches a plateau) [19]. The hardness versus load curve is shown in Figure **5**. In our case, the hardness decreases from 54 GPa (at a load of 2 kgf) and 47 GPa (at a load of 2.5 kgf) to 25 GPa (at a load of 5 kgf).

Figure **5** highlights the characteristic differences in microstructural behavior and mechanics between BL and BH cBN composites, particularly addressing the varied response to applied indentation loads. These differences are crucial for tailoring material properties to specific applications. BL materials, with their higher additive content, experience greater microcracking at indentation corners, contributing to the observed decline in hardness at higher loads.

In contrast, BH materials, due to their higher cBN concentration, maintain consistent hardness. The critical influence of additive type and volume fraction is evident in shaping the fracture toughness and hardness of these materials, making this analysis vital for optimizing cBN composites in advanced cutting tool applications. Evaluating these mechanical properties expands the scope for designing tools for diverse machining conditions, balancing fracture toughness and wear resistance without compromising long-term performance.

The fracture toughness value of the obtained material is 3.27-3.8 MPa*m$^{0.5}$. Unlike hardness, the fracture toughness, calculated according to the Niihara equation [15], is approximately independent of the indenter load and can be measured at any load in the range from 1 kgf to 5 kgf.

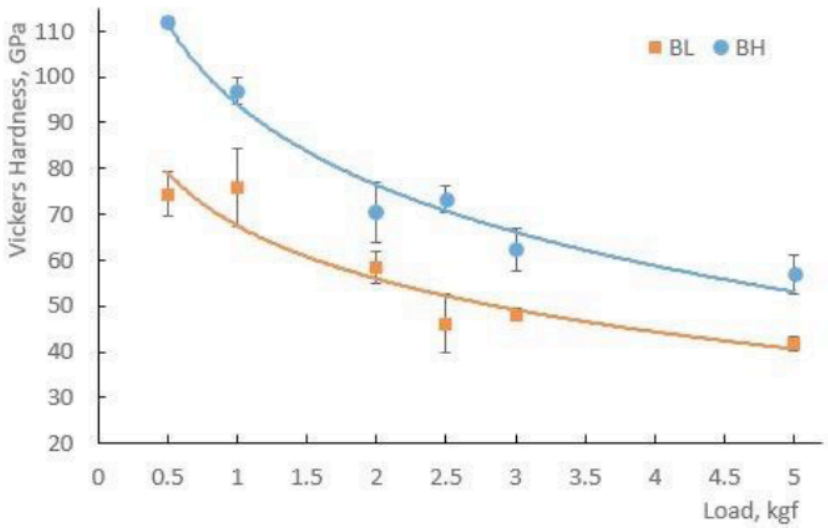

Figure 5: Relationship of Vickers hardness to the applied load on the indenter for the investigated materials.

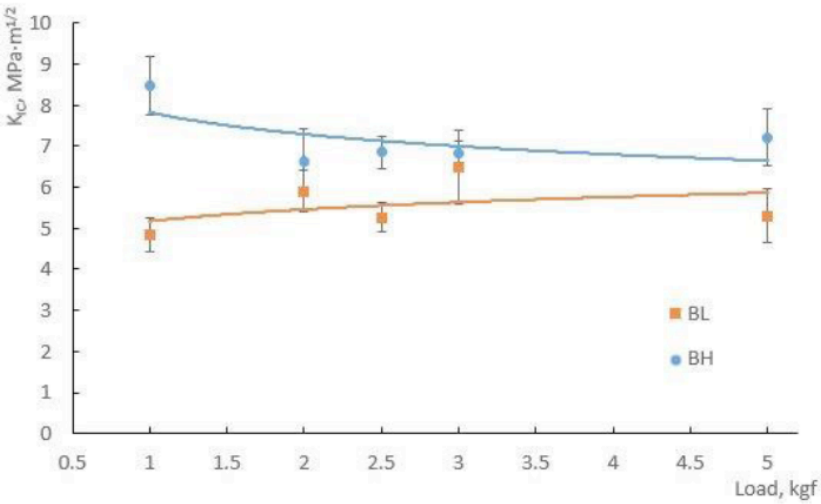

Figure 6: Relationship of fracture toughness (MPa) to the load on the Vickers indenter for BL- and BH- materials.

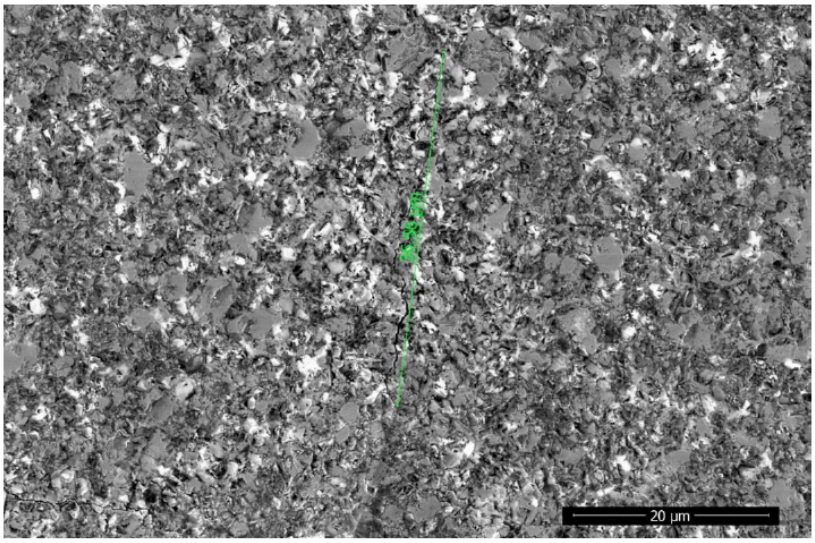

Figure 7: SEM image of the crack in BL material. Load 5 kgf. Magnification 2500x.

In conclusion, the fracture toughness of cBN composites, as determined through the Niihara equation, is shown to remain relatively constant across the tested load range for both BL and BH materials, indicating minimal load dependence. However, the fracture mechanisms differ significantly between the two groups due to variations in composition.

BL materials, with their lower cBN content (46 vol.%) and higher additive content, exhibit more clearly seen microcracking at the indentation corners, which contributes to their slightly lower fracture toughness. In contrast, BH materials, with a higher cBN concentration (82 vol.%) and fewer additives, demonstrate a more robust structure with limited microcracking, resulting in consistently higher fracture toughness

4. DISCUSSION

Many studies report the fact, that the hardness of a particular ceramic material depends on the applied load, the values of the hardness at low loads are bigger, than at high loads. Extensive research over the last decade has sought to explain this phenomenon, known as the "indentation size effect (ISE)" [20]. The most common research links this effect to experimental errors arising from the limitations of the objective lens resolution and the sensitivity of load cells [21, 22]. Bückle [21] suggested that ISE is directly related to the internal structural factors of the tested materials, including elastic recovery during indentation, work hardening during indentation, and the pinning of surface dislocations [23]. It has been observed that dislocation and twinning activity can lead to ISE in alumina ceramics with different grain sizes. Furthermore, crack formation and a small grain size-to-indentation size ratio [24] have been proposed as other explanations for ISE.

Several empirical or semi-empirical equations have been proposed to describe the change in indentation

size depending on the applied test load, including Meyer's law [25], which expresses the relationship between load and indentation size according to equation (3):

$$P = A \times d^n, \quad (3)$$

where the exponent "n" (Meyer's index) is a measure of ISE, and "A" is a constant. The parameters "n" and "A" can be obtained directly from the approximation of the experimental data curve. When n < 2, ISE behavior is observed, and when n = 2, hardness is independent of the applied load.

On the other hand, ISE behavior can be described by the proportional sample resistance (PSR) model [26], where it is assumed that the resistance to residual deformation increases linearly with the indentation size and is directly proportional to PSR. Described by the coefficients "a_1" and "a_2," the ratio "P/d" to "d" can be easily estimated using linear regression. The applicability of the PSR model to describe the observed ISE over a wider range of applied test loads can be verified by checking the linearity between "P/d" and "d," determined by equation (4):

$$\frac{P}{d} = a_1 + a_2 \times d, \quad (4)$$

where "a_1" and "a_2" need to be calculated based on the graphs of the dependence of "P/d" on "d".

According to Li and Bradt [26], the parameters "a_1" and "a_2" can be related to the elastic and plastic properties of the tested material, respectively. In particular, "a_2" has been proposed as a measure of the so-called true hardness, *i.e.*, the load-independent hardness, which can be calculated using equation (5):

$$H_{V_0} = 1.8544 \times a_2 \quad (5)$$

In conclusion, the influence of load on the measured hardness of ceramic materials, including the indentation size effect (ISE), is a phenomenon driven by both experimental factors and intrinsic material properties. The ISE, characterized by decreasing hardness with increasing load, is effectively described using models such as Meyer's law and the proportional sample resistance (PSR) model. Meyer's index (n) provides a quantitative measure of ISE, where deviations from n = 2 indicate load dependence, while the PSR model offers an alternative method to quantify true hardness through the coefficient "a_2." These models highlight the relationship between elastic and plastic properties, dislocation behavior, grain size, and crack formation.

Meyer's Law

Table **2** presents the parameters of Meyer's law, determined using regression analysis of the results for BL and BH materials, shown in Figure **8**.

Table 2: Results of Regression Analysis According to Meyer's Law

Sample	Vickers Hardness		
	n	A	R^2
BL	1.671	3.92	0.9998
BH	2.043	4.58	0.9974

The most significant ISE was observed in the BL material (n = 1.671), while ISE in the BH material (n = 2.043) was not observed. Gong *et al*. [27] studied ISE for various ceramics at indentation loads from 5 to 50 N and found "n" values ranging from 1.748 to 1.979.

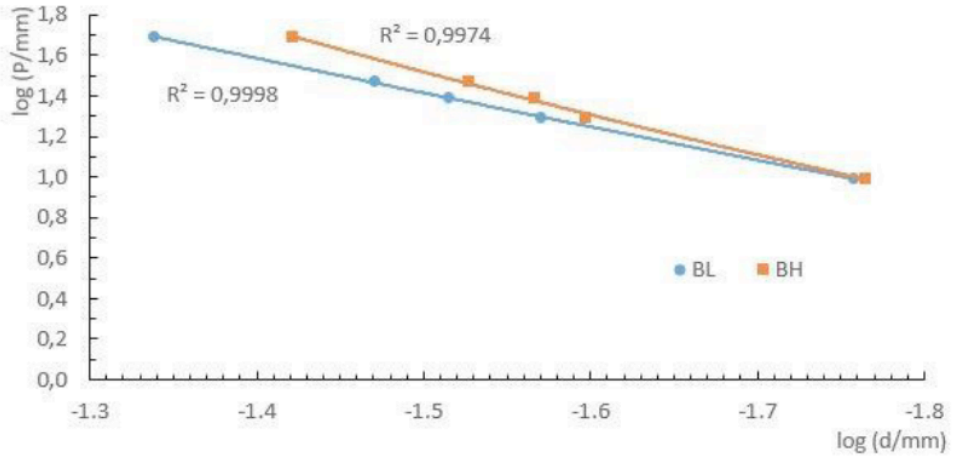

Figure 8: Dependency of log P on log d according to Meyer law for BL- and BH- materials.

Microcracks were detected at the corners of the indentations for all investigated materials across the entire range of applied loads. In their opinion, such microcracking affects the calculated hardness value since part of the energy expended on creating the indentation will be dissipated during crack formation. Berriche and Holt [28] investigated the effect of load on the hardness of hot isostatically pressed Si_3N_4 ceramics of different densities. They found that for high-density/hardness materials, cracks form at the corners of the indentations, starting from the lowest load, *i.e*., 1 N. Our calculated "n" values are in good agreement with the results of Gong *et al*. [27]. In cubic boron nitride-based ceramics, the formation of microcracks in the range of 1 to 5 μm was observed. Figure **6** shows the formation of so-called "ring" indentation cracks in the BL material at 5 kgf with a Vickers indenter. Avoiding the influence of microstructure on hardness values in the range of low loads, where ISE is significant, seems impossible.

PSR Model

Figure **9** shows the "P/d – d" curves for the tested materials. The best-fit parameter values are given in Table **2**. The true hardness (H_{V0}, GPa) was calculated for each material. The results are also given in Table **3**.

Table 3: Results of the Best fit of the PSR Model Parameters

Sample	Vickers Hardness			
	a_1	a_2	H_{V0}, GPa	R^2
BL	228.613	18827.825	34.91	0.9968
BH	-184.442	41234.753	76.46	0.999

The true hardness values for BL and BH materials are: 34.91 GPa for BL material; 76.46 GPa for BH material. These indicators are in good agreement with the Vickers hardness calculations for the investigated materials. The Meyer's method and the PSR model can be used to calculate the true hardness of composite materials for various applications.

Our data suggests that fracture toughness in cBN composites is primarily governed by the cBN content and the nature of the additive phases, rather than the applied load.

In conclusion, the fracture toughness of cBN composites is largely independent of load but heavily influenced by composition. BL materials, with lower cBN content and more additives, exhibit pronounced microcracking and slightly lower toughness, while BH materials, with higher cBN content, demonstrate superior fracture resistance. These findings emphasize the critical role of cBN concentration and additive optimization in enhancing toughness for high-performance applications.

CONCLUSIONS

This study investigated the load dependence of hardness and fracture toughness in cubic boron nitride (cBN) materials of BL and BH groups, differing in additive content.

The results revealed a significant indentation size effect (ISE) in BL materials (lower cBN content, 46 vol%), with hardness decreasing with increasing load, as modeled effectively by both Meyer's law (n = 1.671) and the proportional strength ratio (PSR) model. In contrast, BH materials (higher cBN content, 82 vol%) exhibited minimal ISE (n = 2.043), indicating load-independent hardness. The true hardness values, calculated using the PSR model, were 34.91 GPa for BL and 76.46 GPa for BH materials.

Fracture toughness, calculated using the Niihara equation, showed minimal load dependence for both groups, remaining relatively constant across the tested load range. Microstructural analysis revealed microcracking, particularly pronounced in BL materials at higher loads, influencing the observed ISE. Both

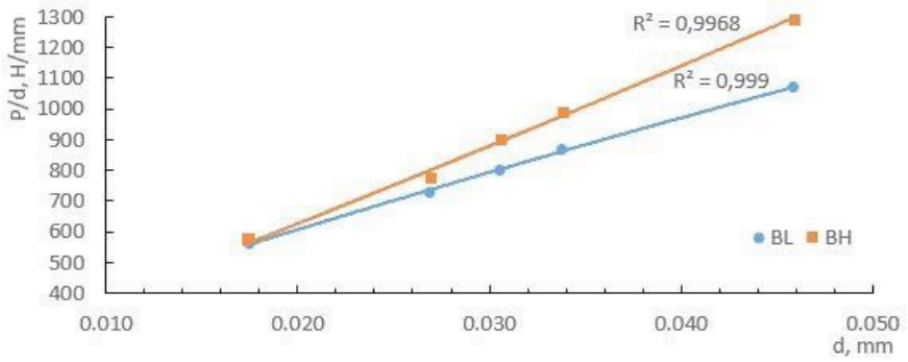

Figure 9: Dependency of P/d on d according to the PSR model for BL- and BH- materials.

Meyer's law and the PSR model proved useful in determining the true hardness of these cBN composites, highlighting the importance of considering ISE when evaluating the hardness of such materials.

The study contributes valuable insights into the mechanical properties and microstructural behavior of cBN-based composites with varying additive concentrations.

DECLARATION OF COMPETING INTEREST

The authors declare that they have no known competing financial interests or personal relationships that could have appeared to influence the work reported in this paper.

ACKNOWLEDGMENTS

Authors are grateful to company “Microbor LLC” for experimental materials and for providing the equipment for the processing of the cutting tools.

REFERENCES

[1] Qian, J. Graphitization of diamond powders of different sizes at high pressure-high temperature / J. Qian, C. Pantea, J. Huang, T. W. Zerda, Y. Zhao // Carbon. – 2004. – V. 42. – P. 2691-2697. https://doi.org/10.1016/j.carbon.2004.06.017

[2] Yin, S. Microstructure and sintering mechanism of sintered cubic boron nitride materials / S. Yin, H. Y. Lai, X. C. Cheng // Chin. Ceram. Soc. – 1984. – V. 12 (4). – P. 450-455.

[3] Sobiyi, K., Sigalas. I, Akdogan, G. & Turan. Y. Performance of mixed ceramics and cBN tools during hard turning of martensitic stainless steel // International Journal of Advanced Manufacturing Technology. — 2015. — T. 77, Ne 5-8. — C. 861-871. https://doi.org/10.1007/s00170-014-6506-z

[4] Slipchenko, K., Turkevich, V., Petrusha, 1, Bushlya, V., Stahl, J.-E. Superhard peBN, materials with chromium compounds as a binder // Procedia Manufacturing. - 2018. - T. 25.-C. 329. https://doi.org/10.1016/j.promfg.2018.06.090

[5] Li Y, Li S, Lv R, *et al*. Study of high-pressure sintering behavior of cBN composites starting with cBN–Al mixtures // J Mater Res. 2008. T. 23. C. 2366-2372. https://doi.org/10.1557/jmr.2008.0316

[6] ISO16462: 2014; Cubic Boron Nitride Inserts, Tipped or Solid. Dimensions, Types. 2014. [Electronic resource] – Access mode: https://www.intechopen.com/online-first/significanceof-boron-nitride-in-composites-and-its-applications - (Accessed: 12.11.2024)

[7] Yu, L. High pressure sintering behavior and mechanical properties of cBN-Ti_3Al and cBN-Ti_3Al-Al composite materials / L. Yu, L. K. Zi, H. K. Wang, *et al*. // High Pressure Res. – 2012. –V. 32 (4). P. 524-531. https://doi.org/10.1080/08957959.2012.736507

[8] Zhang, L. L. cBN-Al-HfC composites: Sintering behaviors and mechanical properties under high pressure / L. L. Zhang, Z. Lv, F. Lin, *et al*. // Int. J. Refract. Met. H. – 2015, – V. 50. – P. 221-226. https://doi.org/10.1016/j.ijrmhm.2015.01.015

[9] Yang, Limin. Compositions, mechanical properties and microstructures of cBN-based composites sintered with Al or TiC / Limin Yang, Zhenming Yue, Jianhong Gong, Xiaodi Zhao, Xingrong Chu // Structural, Functional and Bioceramics. – 2017. – V. 116. – 2017. P. 254-259. https://doi.org/10.1080/17436753.2017.1290330

[10] Zhang L, Lin F, Lv Z, *et al*. cBN–Al–HfC composites: sintering behaviors and mechanical properties under high pressure. Int J Refract Met Hard Mat. – 2015. – V. 50. P. 221-226. https://doi.org/10.1016/j.ijrmhm.2015.01.015

[11] Barry J, Byrne G. Cutting tool wear in the machining of hardened steels: part II: cubic boron nitride cutting tool wear. Wear. – 2001. – V. 247. P. 152–160. https://doi.org/10.1016/S0043-1648(00)00528-7

[12] Chiou S, Ou S, Jang Y, *et al*. Research on cBN/TiC composites. Part1: effects of the cBN content and sintering process on the hardness and transverse rupture strength. Ceram Int. – 2013. – V. 39. P. 7205-7210. https://doi.org/10.1016/j.ceramint.2013.02.066

[13] Turkevych D.V., Bushlya V., Stahl J.E., *et al*. HPHT sintering, microstructure, and properties of B_6O- and TiC-containing composites based on cBN. J Superhard Mater. – 2015. – V. 37. P. 143-154. https://doi.org/10.3103/S1063457615030016

[14] S. J. Bull, T. F. Page, E. H. Yoffe. An explanation of the indentation size effect in ceramics // Philosophical Magazine Letters. 1989. V. 59, I. 6. P. 281 – 288. https://doi.org/10.1080/09500838908206356

[15] Niihara K. Evaluation of K_{Ic} of brittle solids by the indentation method with low crack-to-indent ratios / K. Niihara, R. Morena, D.P.H. Hasselman // Journal of Materials Scince. V. 1. 1982. P. 13-16. https://doi.org/10.1007/BF00724706

[16] Lawn B.R. Equilibrium penny-like cracks in indentation fracture / B.R. Lawn, E.R. Fuller // Journal of Materials Science. V. 10 (12). 1975. P. 2016-2024. https://doi.org/10.1007/BF00557479

[17] Tanaka K., Elastic/plastic indentation hardness and indentation fracture toughness: the inclusion core model // Journal of Materials Science. V. 22, I. 4. 1987. P. 1501-1508. https://doi.org/10.1007/BF01233154

[18] Klimczyk P. Cubic boron nitride based composites for cutting applications / P. Figiel, I. Petrusha, A. Olszyna // Journal of Achievements in Materials and Manufacturing Engineering. V. 44. 2011. P. 198-204

[19] Karsten Durst, Björn Backes, Oliver Franke, Mathias Göken. Indentation size effect in metallic materials: Modeling strength from pop-in to macroscopic hardness using geometrically necessary dislocations // Acta Materialia. V. 54. I. 9. 2006. P. 2547-2555. https://doi.org/10.1016/j.actamat.2006.01.036

[20] J. Andrejovska, J. Dusza: Hardness and Indentation Load/Size Effect in Silicon based Ceramics // in Proc. of the NANOCON. Rožnov pod Radhoštem, Chech Republic. 2009.

[21] Bückle, I., H. Process in Micro-Indentation Hardness Testing // Metall. Rev. 1959. V. 4. P. 49-100. https://doi.org/10.1179/095066059790421746

[22] Mason, W., Johnson, P. F., Varner, J., R. Importance of Load Cell Sensitivity in Determination of the Load Dependence of Hardness in Recording Microhardness Tests // J. Mater. Sci. 1991. V. 26. P. 6576-6580. https://doi.org/10.1007/BF00553680

[23] Tarkanian, M., L., Neumann, J., P., Raymond, L. In The Science of Harndness Testing and Its Research Applications // ed. J. H.Westbrook and H. Conrad. American Society for Metals. Metal Park. OH. 1973.

[24] Li, H., Bradt, R., C. // J. Mat. Sci. 1996. V. 31. P. 1065-1070. https://doi.org/10.1007/BF00352908

[25] Tabor, D. The hardness of Metals // Oxford University Press. Oxford. UK. 1951

[26] Li, H., Bradt, R. C. // J. Mater. Sci. 1993. V. 28. P. 917-926. https://doi.org/10.1007/BF00400874

[27] Gong, J., Wu, J., Guan, Z. Examination of the indentation size effect in low-load vickers hardness testing of ceramics // J. Eur. Ceram. Soc. 1999. V. 19, I. 15. P. 2625-2631. https://doi.org/10.1016/S0955-2219(99)00043-6

[28] Berriche, R., Holt, R. T. Effect of load on the hardness of tot isostatically pressed silicon nitride // J. Am. Cearm. Soc. 1993. V. 76, I. 6. P. 1602-1604. https://doi.org/10.1111/j.1151-2916.1993.tb03946.x

Received on 22-11-2024 Accepted on 26-12-2024 Published on 31-12-2024

https://doi.org/10.31875/2410-4701.2024.11.13